TWO-DIMENSIONAL LIQUID COLUMN AND LIQUID DROPLET IMPACT ON A SOLID WEDGE

by G. X. WU

(*Department of Mechanical Engineering, University College London, Torrington Place, London* WC1E 7JE, *UK*)

[Received 27 June 2007. Revise 1 August 2007. Accepted 2 August 2007]

Summary

The hydrodynamic impact due to a two-dimensional (2D) liquid column or a 2D liquid droplet hitting on a solid wedge is analysed. The problem is solved using the complex velocity potential together with the boundary element method. A stretched coordinate system is used, which is defined through the ratio of the normal Cartesian coordinate system to an appropriately chosen time-varying length scale. Numerical simulations are first made for impact by a liquid wedge. The results from the time-domain method are found to be in a good agreement with the similarity solution. Simulations are also made for impact by an elliptic droplet. A condition for bisection of the droplet is introduced, which is found to provide stable and converged results.

1. Introduction

Fluid–structure collision at high speed can be found in many engineering applications. Well-known examples include green water on a ship deck, slamming, wave impact on offshore platforms and the coastline, as well as impact of super-cooled large droplets and ice lumps in the aeronautical setting, and applications in sports. An extreme example is the impact caused by a tsunami, which can create large-scale devastation.

A solid wedge is often used in mathematical and numerical modelling for impact, especially in the context of water entry. Typical examples include a rigid wedge entering water at constant speed. This problem was solved by Dobrovol'skaya (**1**) based on the self-similar method and by Zhao and Faltinsen (**2**) based on the time-domain method. Lu *et al.* (**3**) considered a similar case with an elastic wedge. The fully nonlinear coupling between the fluid flow and the wedge deflection was tackled through a semi-implicit scheme for the Bernoulli equation. Wu *et al.* (**4**) considered the water entry problem of a rigid wedge in free fall motion. The mutual dependence between the body acceleration and the fluid flow was decoupled through the use of an auxiliary function (**5**). More recently, Wu (**6**) considered the water entry problem of rigid twin wedges at constant speed through a three-stage approach. A closely related problem is the impact by a liquid wedge on a solid wall, which was solved based on the self-similar method by Cumberbatch (**7**).

A common feature in the above problems is that the liquid has a flat surface. In many other cases, however, such as impact by a steep water wave or by a liquid droplet on a structure, the liquid surface has curvature. A problem of this kind was solved by Wu (**8**) when he considered liquid column with curved surface hitting on a flat rigid surface. A significant point noticed by him was that the choice of the length scale used for the stretched coordinate system was crucial in the numerical solution.

⟨gx_wu@meng.ucl.ac.uk⟩. Cheung Kong and Long Jiang Visiting Professor, College of Shipbuilding College, Harbin Engineering University, Harbin 150001, People's Republic of China

Q. Jl Mech. Appl. Math, Vol. 60. No. 4
Advance Access publication 27 September 2007. doi:10.1093/qjmam/hbm020

A similar problem was solved analytically by Howison *et al.* (**9**) and Purvis and Smith (**10**) when they used the small time expansion method and considered impact of a liquid droplet on a flat surface covered by a thin layer of fluid.

In this work, we shall consider the problem of impact by a liquid with a curved surface on a rigid wedge. As it has been pointed out (**4**, **6**, **8**), a unique feature of this fluid–structure impact problem is that the collision usually starts from a single contact point. At the initial stage of the impact, the significant effect of the impact on the fluid flow will be confined in a small region near the contact point. Within this region, the physical parameters, including velocity and pressure, can change rapidly. An ideal approach for this kind of problem is to use a stretched coordinate system (ξ, η), defined through the ratio of the Cartesian system (x, y) over a time-dependent length scale $s(t)$, or $(\xi, \eta) = (x/s, y/s)$. This method was used in (**4**, **6**, **8**), and it was one of the major reasons for the success of those analyses. A common feature of $s(t)$ in these applications is that it is a monotonic function of t, and it has to be suitably chosen for each problem. Here, we will also choose a monotonic function for the length scale but with an upper limit s_0 based on $s_0/d \gg 0$, where d is the typical length scale of the problem, such as the size of the droplet. This means if $s(t) > s_0$ when $t > t_0$, we will simply take $s(t) = s_0$. One reason for this choice is that when the length scale is not a small quantity, the distinction between (ξ, η) and (x, y) diminishes and a time-independent length scale will make the analysis simpler. Another reason is that when a droplet hits a wedge, one can expect that it will be bisected eventually. When that happens, the advantage of a time-dependent stretched system disappears.

In the following sections, we will first outline the mathematical equations and the numerical method. This is followed by the numerical results. The first example considered is the collision between a solid wedge and a liquid wedge. The flow in this case is self-similar. This allows us to compare the numerical results from the similarity solution and the time-domain solution. We then consider the impact of a liquid droplet of elliptical shape on the wedge. The numerical simulation is made over a sufficiently long period that covers the bisection of the droplet.

2. Governing equations and numerical procedure

We consider the hydrodynamic problem of a liquid column or a liquid droplet moving towards a solid wedge with speed $-U$. This is dynamically equivalent to the problem of a wedge moving with speed U towards the stationary liquid, as shown in Fig. 1. A Cartesian coordinate system (O, x, y) is defined in which x is in the direction of motion and the origin is located at the initial contact point

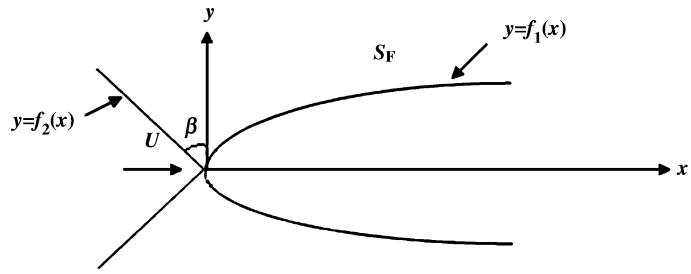

Fig. 1 Sketch of collision between a solid wedge and a two-dimensional liquid column

during the impact. The fluid is assumed to be incompressible and inviscid, and the flow is assumed to be irrotational. A velocity potential ϕ can then be introduced, which satisfies

$$\nabla^2\phi = 0 \tag{2.1}$$

in the fluid domain R. On the body surface S_0, we have

$$\frac{\partial\phi}{\partial n} = Un_x,$$

where $n = (n_x, n_y)$ is the normal vector of the body surface pointing out of the fluid domain. The Lagrangian form of the kinematic and dynamic conditions on the free surface S_F or $y = \zeta$ can be written as

$$\frac{dx}{dt} = \frac{\partial\phi}{\partial x}, \quad \frac{dy}{dt} = \frac{\partial\phi}{\partial y}, \tag{2.2}$$

$$\frac{d\phi}{dt} = \frac{\partial\phi}{\partial t} + \nabla\phi\cdot\nabla\phi = \frac{1}{2}\nabla\phi\cdot\nabla\phi. \tag{2.3}$$

Without loss of generality (see, for example, (**8**, Conclusions)), we can assume that both the solid surface and the liquid is symmetric about $y = 0$. Thus, we have $\partial\phi/\partial y = 0$ on $y = 0$. Furthermore at the moment of contact $t = 0$, the shape of the liquid is assumed as $y = f_1(x),\ x \geqslant 0$, and that of the solid face is

$$y = f_2(x) = -\frac{x}{\tan\beta}, \quad x \leqslant 0,$$

where $f_1(x)$ is single valued and β is the deadrise angle as shown in Fig. 1.

When a time-dependent length scale s is chosen, we can write

$$\phi(x, y, t) = Us\varphi(\xi, \eta, t),$$

where $\xi = x/s$ and $\eta = y/s$. Equation (2.1) obviously has the same form in the stretched system, while (2.2) and (2.3) become

$$\frac{d(s\xi)}{dt} = U\frac{\partial\varphi}{\partial\xi}, \quad \frac{d(s\eta)}{dt} = U\frac{\partial\varphi}{\partial\eta}, \tag{2.4}$$

$$\frac{d(s\varphi)}{dt} = \frac{U}{2}(\varphi_\xi^2 + \varphi_\eta^2). \tag{2.5}$$

Similarly, the undisturbed liquid surface and the body surface become

$$\eta_1 = \frac{1}{s}f_1(s\xi), \quad \eta_2 = \frac{1}{s}f_2(s\xi - Ut).$$

To solve the above velocity potential problem, it is convenient to adopt the complex potential $w = \varphi + i\psi$, where ψ is the stream function. The method has been previously used in many free-surface-related problems (**4** to **6**, **8**, **11** to **13**). It is based on Cauchy's theorem which gives

$$\oint \frac{w}{z - z_0}dz = 0, \tag{2.6}$$

where $z = \xi + i\eta$ and z_0 is a point outside the fluid domain R. The integration in (2.6) is along the fluid boundary. On the fluid boundary, we divide the surface into segments with n nodes. The complex function can be written in terms of the interpolation function

$$w = \sum_{j=1}^{n} w_j N_j(z), \tag{2.7}$$

where w_j is the value of the complex potential on node j. When linear interpolation is used, we have

$$N_j(z) = \begin{cases} (z - z_{j+)})/(z_j - z_{j+1}), & z \in (z_j, z_{j+1}), \\ (z - z_{j-1})/(z_j - z_{j-1}), & z \in (z_{j-1}, z_j), \\ 0, & z \notin (z_{j-1}, z_{j+1}). \end{cases} \tag{2.8}$$

Substituting (2.7) and (2.8) into (2.6), letting z_0 approach node z_k and using the boundary conditions, we have

$$\sum_{j=1}^{n} A_{kj}\varphi_j|_{j\in S_0+S_C} + i\sum_{j=1}^{n} A_{kj}\varphi_j|_{j\in S_F} = -\sum_{j=1}^{n} A_{kj}\varphi_j|_{j\in S_F} - i\sum_{j=1}^{n} A_{kj}\varphi_j|_{j\in S_0+S_C}, \tag{2.9}$$

where

$$A_{kj} = \frac{z_k - z_{j-1}}{z_j - z_{j-1}} \ln\frac{z_j - z_k}{z_{j-1} - z_k} + \frac{z_k - z_{j+1}}{z_j - z_{j+1}} \ln\frac{z_{j+1} - z_k}{z_j - z_k},$$

in which the two singularities when $k = j$ on the right-hand side cancel each other.

In (2.9), the terms on the right-hand side are known from the boundary conditions, while the terms on the left are unknown. At the intersection of the free surface and the body surface in particular, both the stream function and the potential are known, and they are both moved to the right-hand side of the equation. In the equation S_C is a control surface far away from the solid boundary.

A common feature during the fluid–structure impact is the development of jet. This is a thin layer of fluid along the body surface, within which the fluid can move very fast. To capture the flow accurately within the jet, elements used there must be small enough, which can increase the CPU and memory requirement dramatically. Also when z_k is on one side of the jet and is close to element (z_j, z_{j+1}) on the other side of the jet, an ill-conditioned matrix can be created. This can increase the number of iterations significantly when the matrix equation is solved. Thus, we use the following procedure to deal with the jet. Assuming element (z_k, z_{k+1}) is on the free surface of the jet, we have

$$\eta = \eta_k + \frac{\eta_{k+1} - \eta_k}{\xi_{k+1} - \xi_k}(\xi - \xi_k)$$

along the free surface of this element. We take a line from (ξ_k, η_k), which is perpendicular to the body surface and intersects the body surface through element (z_j, z_{j+1}). Because the jet is very thin, we can write the potential as

$$\varphi = A + B\xi + C\eta, \tag{2.10}$$

corresponding to element (z_k, z_{k+1}). The free surface boundary condition then gives

$$\varphi_k = A + B\xi_k + C\eta_k, \quad \varphi_{k+1} = A + B\xi_{k+1} + C\eta_{k+1},$$

and the body surface boundary condition gives

$$-B(\eta_{j+1}-\eta_j)+C(\xi_{j+1}-\xi_j)=-(\eta_{j+1}-\eta_j).$$

Thus, we have

$$B=\frac{(\varphi_{k+1}-\varphi_k)(\xi_{j+1}-\xi_j)+(\eta_{k+1}-\eta_k)(\eta_{j+1}-\eta_j)}{(\xi_{k+1}-\xi_k)(\xi_{j+1}-\xi_j)+(\eta_{k+1}-\eta_k)(\eta_{j+1}-\eta_j)},$$

$$C=\frac{(\varphi_{k+1}-\varphi_k)(\eta_{j+1}-\eta_j)-(\eta_{j+1}-\eta_j)(\eta_{k+1}-\eta_k)}{(\xi_{k+1}-\xi_k)(\xi_{j+1}-\xi_j)+(\eta_{k+1}-\eta_k)(\eta_{j+1}-\eta_j)}.$$

Corresponding to (2.10), we can write

$$\psi=D-C\xi+B\eta,$$

in which D can be obtained from

$$D=\psi_j+C\xi_j-B\eta_j$$

on the body surface. We then obtain on the free surface

$$\psi_k=D-C\xi_k+B\eta_k.$$

As a result, both the potential and stream function are known on node z_k, and they can both be moved to the right-hand side of (2.9).

We then draw a line from node z_j in the normal direction of the body surface. Assume that this line intersects the free surface at z_s, where the potential φ_s can be found through the free surface boundary condition. Using the body surface boundary condition, we have

$$\varphi_j=\varphi_s+\sqrt{(x_s-x_j)^2+(y_s-y_j)^2}\frac{\partial\varphi_j}{\partial n}. \tag{2.11}$$

This means that both the potential and the stream function on node j become known and they can be moved to the right-hand side of (2.9). The procedure above shows that there will be no unknowns on both sides of the jet. Thus, the existence of the jet will not increase the scale of the computation significantly.

When the solution of (2.9) has been found, the pressure can in theory be obtained from the Bernoulli equation

$$p=-\rho\phi_t-\frac{1}{2}\rho(\phi_x^2+\phi_y^2).$$

The difficulty is that ϕ_t is in fact still not known directly. It nevertheless is another harmonic function as it satisfies Laplace's equation. On the free surface, $p=0$ gives

$$\phi_t=-\frac{1}{2}(\phi_x^2+\phi_y^2). \tag{2.12}$$

On the body surface, we have (**14**)

$$\frac{\partial \phi_t}{\partial n} = -U \frac{\partial \phi_x}{\partial n}. \tag{2.13}$$

To solve the boundary-value problem for ϕ_t the stretched coordinate system can also be used. In fact, we can write $\phi_t = U^2 \chi(\xi, \eta, t)$. Equations (2.12) and (2.13) then become

$$\chi = -\frac{1}{2}(\varphi_\xi^2 + \varphi_\eta^2),$$
$$\frac{\partial \chi}{\partial n} = -\frac{\partial \varphi_\xi}{\partial n}, \tag{2.14}$$

respectively. Similar to the procedure used for φ, we can define a complex potential $w = \chi + i\omega$ and rewrite the boundary condition on the body surface in (2.14) as

$$\omega = \varphi_\eta.$$

This complex potential can then be solved in the exactly same way as that for $\varphi + i\psi$.

To treat χ in the jet, we can use the normal derivative of the pressure on the body surface. We have

$$\frac{1}{\rho}\frac{\partial p}{\partial n} = -\frac{\partial \phi_t}{\partial n} - \phi_x \frac{\partial \phi_x}{\partial n} - \phi_y \frac{\partial \phi_y}{\partial n}.$$

Since $f_{2x} = -n_x/n_y$, this equation becomes

$$\begin{aligned}\frac{1}{\rho}\frac{\partial p}{\partial n} &= n_y[U(-f_{2x}\phi_{xx} + \phi_{xy}) - \phi_x(-\phi_{xx} f_{2x} + \phi_{xy}) - \phi_y(-\phi_{xy} f_{2x} + \phi_{yy})] \\ &= n_y[\phi_{xx}(-U f_{2x} + \phi_x f_{2x} + \phi_y) + \phi_{xy}(U - \phi_x + \phi_y f_{2x}).\end{aligned} \tag{2.15}$$

The body surface boundary condition on ϕ can be written as

$$\phi_y = (\phi_x - U) f_{2x}. \tag{2.16}$$

Differentiating this equation with respect to x along the body surface, we obtain

$$\phi_{xy}(1 - f_{2x}^2) = (\phi_x - U) f_{2xx} + 2\phi_{xx} f_{2x}. \tag{2.17}$$

Substituting (2.16) and (2.17) into (2.15), we have

$$\frac{1}{\rho}\frac{\partial p}{\partial n} = -(\phi_x - U)^2 n_y f_{2xx}.$$

It is important to note that this equation has been derived for general cases. Thus, it is valid even for a solid body of curvature. For a wedge, we have $f_{2xx} = 0$ and therefore $\partial p/\partial n = 0$. In a way similar to that in (2.11) we can then write

$$p_j = p_s.$$

Since $p_s = 0$ on the free surface, we obtain

$$\frac{\partial \phi_j}{\partial t} = -\frac{1}{2}\nabla\phi_j \cdot \nabla\phi_j.$$

This gives

$$\chi_j = -\frac{1}{2}\nabla\varphi_j \cdot \nabla\varphi_j \tag{2.18}$$

on the body surface attached to the jet. On the free surface of the jet, we use an equation similar to (2.11) to obtain

$$\begin{aligned}\omega_s &= \omega_j - \sqrt{(x_s - x_j)^2 + (y_s - y_j)^2}\frac{\partial \omega_j}{\partial n} \\ &= \omega_j - \sqrt{(x_s - x_j)^2 + (y_s - y_j)}\frac{\partial \chi_j}{\partial s},\end{aligned}$$

where the partial derivative of χ is taken along the body surface based on (2.18), or along the direction obtained by rotating the normal of the surface 90 degrees clockwise.

Once χ is found, the force F on the wedge can be found from

$$\begin{aligned}\mathrm{F} &= -\rho \int_{S_0} \left(\phi_t + \tfrac{1}{2}\nabla\phi \cdot \nabla\phi\right) n_x dS|_{(x,y)} \\ &= \rho U^2 s \int_{S_0} \left(\chi + \tfrac{1}{2}\nabla\varphi \cdot \nabla\varphi\right) n_\xi dS|_{(\xi,\eta)}.\end{aligned}$$

3. Numerical results

The boundary of the fluid domain in the stretched coordinate system is first divided into small panels. The problem is then solved based on the procedure described in section 2. Time-stepping method based on (2.4) and (2.5) is used to follow the variation of the wetted surface of the wedge and the deformation of the free surface. When the neighbouring nodes become too close or too far apart, regridding is applied and interpolation is used to obtain results on new nodes from old ones. The sizes of panels and the time steps have been reduced systematically until the convergence of the pressure and the free surface profile have been achieved.

3.1 *Impact by a liquid wedge on a solid wedge*

We first consider the case in which the solid wedge collides with a liquid wedge. The length scale for the stretched coordinate system is chosen as $s = Ut$. This problem is self-similar, which means that φ is not a function of t in the stretched coordinate system. The similarity solution can be obtained through a numerical procedure in (**4**, **6**, **8**) and the results are used below for comparison with the time-domain solution.

At the moment of impact, the liquid surface is defined as

$$y = f_1(x) = x \tan\gamma.$$

The time marching can be achieved through s if we rewrite (2.4) and (2.5) as

$$\frac{d(s\xi)}{ds} = \frac{\partial\varphi}{\partial\xi}, \quad \frac{d(s\eta)}{ds} = \frac{\partial\varphi}{\partial\eta},$$

$$\frac{d(s\varphi)}{ds} = \frac{1}{2}(\varphi_\xi^2 + \varphi_\eta^2).$$

Three cases with $\beta = 45^\circ, 30^\circ, 10^\circ$ ($\gamma = 90^\circ - \beta$), respectively, are considered. The initial s is taken as 10^{-3} and the time-domain solution given in Figs 2 to 4 corresponding to $s = 1$. It can be seen that in all these three cases, the results from the similarity solution and the time-domain solution are in good agreement. The disturbance to the liquid surface profile is mainly confined to an area near the body. When β is small, a jet can be developed along the body surface. The pressure, which is non-dimensionalized by ρU^2, increases significantly near the jet then drops sharply to the ambient pressure. This is similar to the results when a wedge enters a flat liquid surface (**4**) and when a liquid wedge hits a flat rigid surface (**8**).

3.2 *Impact by a liquid droplet on the solid wedge*

We next consider the case in which the solid wedge collides with an elliptical liquid droplet. At the moment of impact, the liquid surface is defined as

$$\frac{(x-a)^2}{a^2} + \frac{y^2}{b^2} = 1.$$

If we consider only the upper half with $y \geqslant 0$, this equation can be written as

$$y = f_1(x) = \lambda\sqrt{2ax - x^2},$$

where $\lambda = b/a$. At time t, we then use $f_1(x_s) = f_2(x_s - Ut)$ to obtain

$$x_s = \frac{Ut + a\lambda^2\tan^2\beta - \lambda\tan\beta\sqrt{a^2\lambda^2\tan^2\beta + (2a - Ut)Ut}}{1 + \lambda^2\tan^2\beta},$$

$$y_s = \frac{(Ut - a)\lambda^2\tan^2\beta + \lambda\tan\beta\sqrt{a^2\lambda^2\tan^2\beta + (2a - Ut)Ut}}{\tan\beta(1 + \lambda^2\tan^2\beta)}.$$

As discussed by Wu (**8**), the choice of $s = Ut$ for this problem would lead to an infinitely large wetted surface in the stretched coordinate system. It would therefore be appropriate to choose $s = y_s$. If we introduce a non-dimensional parameter

$$r = \frac{s}{a} = \frac{(\tau - 1)\lambda^2\tan^2\beta + \lambda\tan\beta\sqrt{\lambda^2\tan^2\beta + (2 - \tau)\tau}}{\tan\beta(1 + \lambda^2\tan^2\beta)}, \tag{3.1}$$

where $\tau = Ut/a$, the equations for the surfaces of the liquid and the wedge become

$$\eta = \frac{\lambda}{r}\sqrt{2r\xi - (r\xi)^2},$$

$$\eta = -\frac{\xi - \tau/r}{\tan\beta}.$$

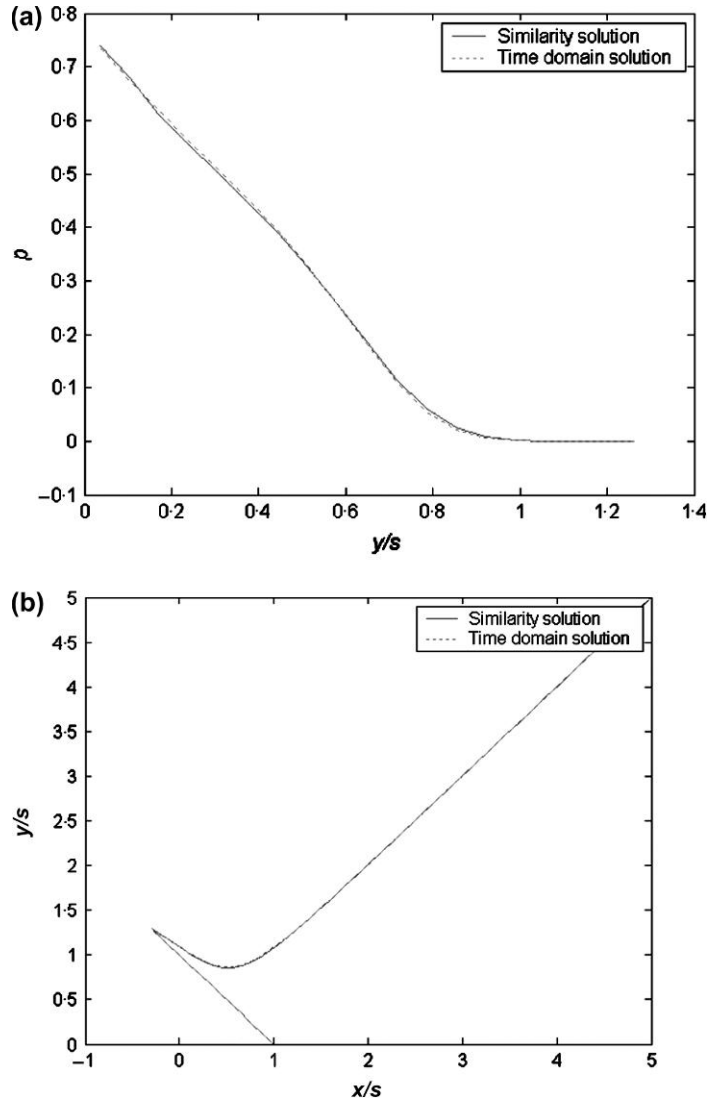

Fig. 2 (a) Pressure distribution along the wedge surface ($\beta = \pi/4, \gamma = \pi/4$). (b) Profile of the liquid surface ($\beta = \pi/4, \gamma = \pi/4$)

The free surface boundary condition in (2.4) and (2.5) can now be written as

$$\frac{d(r\xi)}{d\tau} = \frac{\partial\varphi}{\partial\xi}, \quad \frac{d(r\eta)}{d\tau} = \frac{\partial\varphi}{\partial\eta},$$

$$\frac{d(r\varphi)}{d\tau} = \frac{1}{2}(\varphi_\xi^2 + \varphi_\eta^2).$$

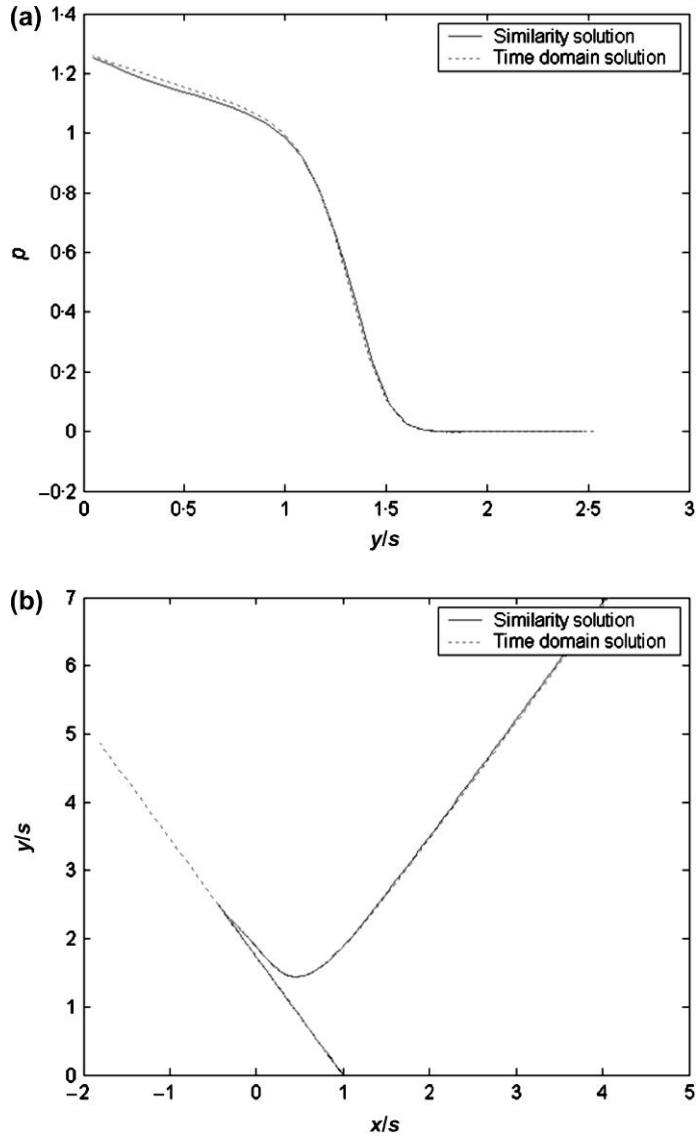

Fig. 3 (a) Pressure distribution along the wedge surface ($\beta = \pi/6$, $\gamma = \pi/3$). (b) Profile of the liquid surface ($\beta = \pi/6$, $\gamma = \pi/3$)

It should be noticed that r in (3.1) increases initially with τ. When it reaches $r = \lambda$, it will then decrease. This corresponds to $\tau = \lambda \tan\beta + 1$. Thus, it would be more appropriate to define

$$r = \begin{cases} y_s/a, & \tau \leqslant \lambda \tan\beta + 1, \\ \lambda, & \tau > \lambda \tan\beta + 1. \end{cases}$$

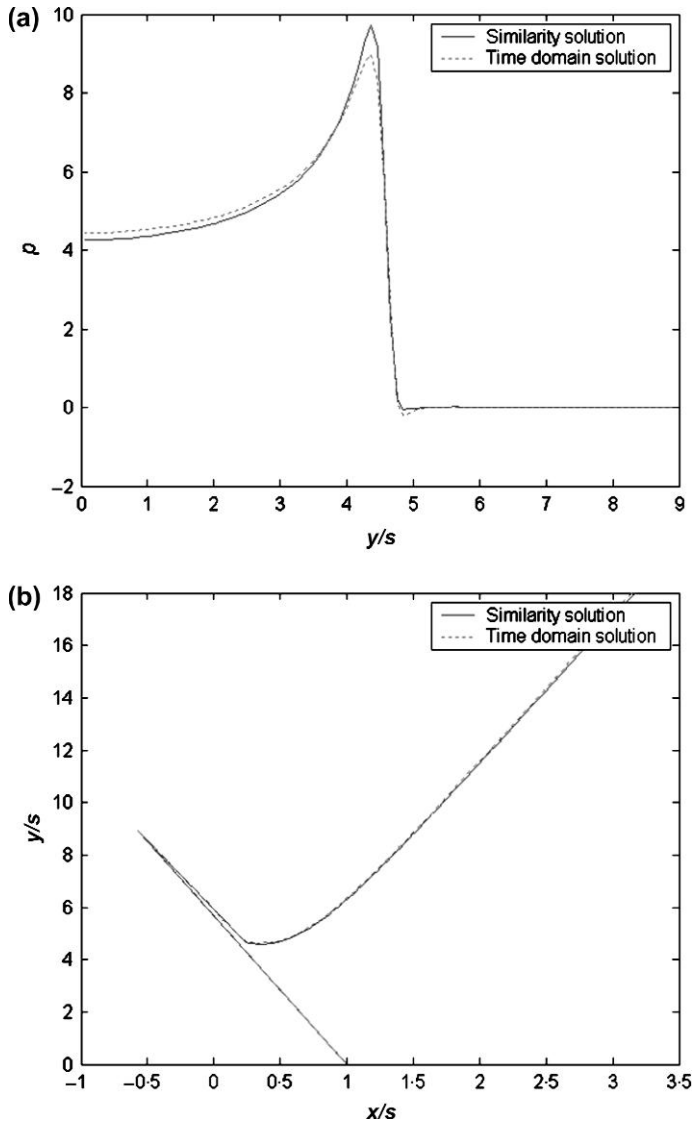

Fig. 4 (a) Pressure distribution along the wedge surface ($\beta = \pi/18, \gamma = 4\pi/9$). (b) Profile of the liquid surface ($\beta = \pi/18, \gamma = 4\pi/9$)

Simulation is first made for the case with $\beta = \pi/4$ and $\lambda = 1$. When the tip of the wedge penetrates the droplet surface at the beginning of the impact, the computational domain covers only small section of the liquid as the disturbance is confined in a small region. When r increases, the computational domain then covers the whole droplet. As r increases further, the tip of the solid wedge becomes closer and closer to the other side of the liquid surface. An assumption is then made

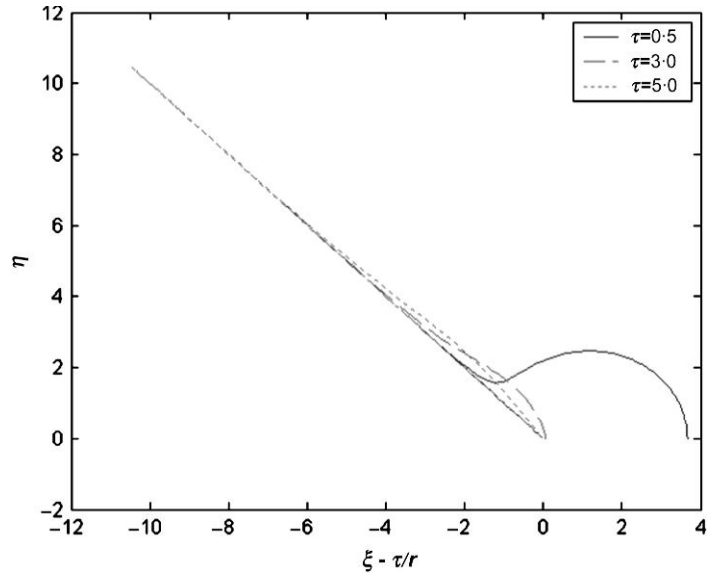

Fig. 5 The surface of a liquid droplet at different time steps after impact ($\lambda = 1$)

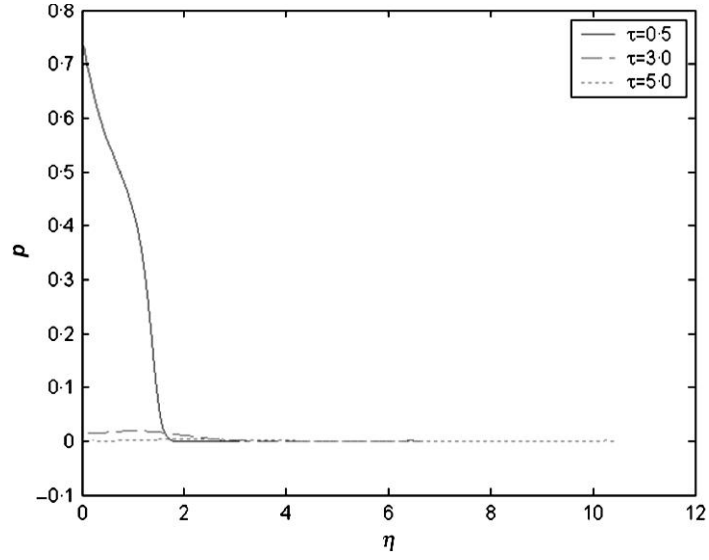

Fig. 6 Pressure distribution over the wedge surface at different time steps ($\lambda = 1$)

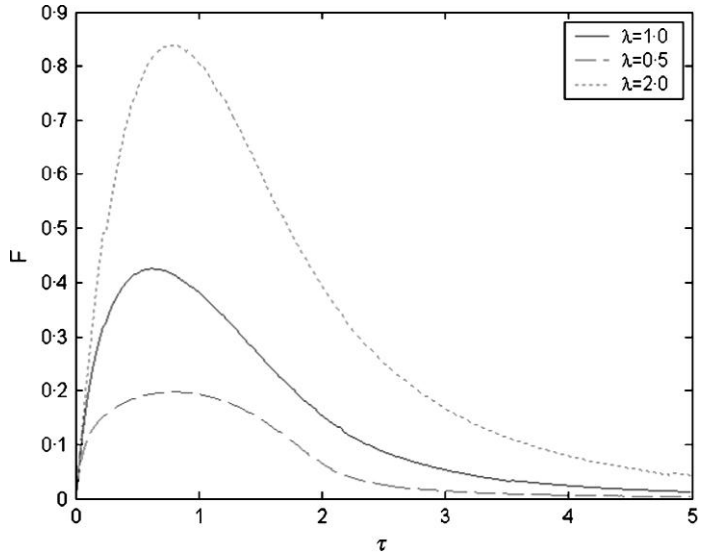

Fig. 7 Force history on the wedge

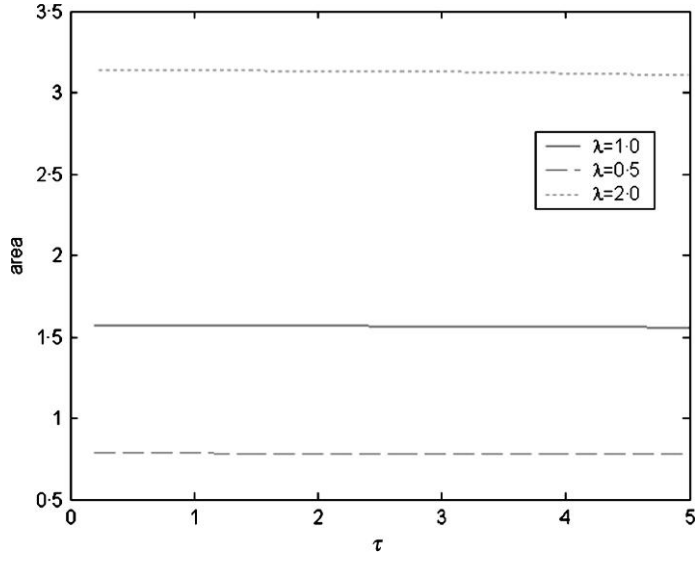

Fig. 8 Area of a liquid droplet after impact

that when the distance between the tip of the wedge and the surface of the liquid Δd is sufficiently small, the element node on the free surface is moved to the tip of the wedge. This node will then slide along the wedge surface in the subsequent simulation.

Figure 5 gives the shape of the liquid surface at three different time steps with $\lambda = 1$. It is assumed when Δd is one per cent of the element size, the bisection of the droplet occurs. This corresponds to $\tau \approx 3{\cdot}53$. Obviously, when a different value is chosen as a condition for the bisection, τ will be different. However, this does not have significance on the numerical results as determined from the liquid surface profile and pressure distribution. Figure 6 gives the pressure distribution non-dimensionalized by ρU^2 over the wedge surface at the same time steps as those in Fig. 5. This shows that the pressure tends to zero as τ increases. This is of course expected. In fact, when the liquid droplet moves towards a wedge, it has limited amount of momentum. When it hits the wedge, its momentum will decline due to the pressure applied by the wedge on the droplet. If the pressure was persistent and did not decay, the momentum in the droplet would become negative.

As τ increases, one may speculate that there could be three possibilities for the motion of the bisected droplet:

(1) there is no motion relative to the wedge;
(2) liquid will slide along the wedge while its shape remains unchanged; and
(3) the droplet will become thinner and thinner and spread more and more widely over the wedge surface. From the result in Fig. 5, it seems that (2.3) is most likely to happen.

Figure 7 gives the force history on the wedge as $\beta = \pi/4$, which is non-dimensionalized by $\rho U^2 a$, due to impact by elliptic droplets with $\lambda = 1, 0{\cdot}5, 2$, respectively. It shows that in these three cases, the force will initially increase with time. When it reaches a peak, it will then decline and tend to zero. When the liquid is longer and thinner, the force is smaller. Otherwise the force is bigger.

To further check the accuracy of the results, Fig. 8 gives area of the droplet. It should remain a constant and equal to $\lambda\pi$. In the figure, curves start at the instant when the whole liquid domain has been included in the computational domain. It can be seen that the mass conservation law is maintained to a high degree of accuracy during the entire simulation. In fact, the largest errors throughout the simulations are 0.78 per cent, 0.56 per cent and 0.96 per cent at $\lambda = 1, 0{\cdot}5$ and 2, respectively.

4. Conclusions

The impact problem by a liquid column and a liquid droplet on a rigid wall has been solved based on the velocity potential theory. When a thin jet is developed, it is treated through a local linear approximation for the potential. As a result, both the velocity potential and the stream function are known within the jet. Therefore, the presence of the jet does not lead to any major difficulty in the computation or any significant increase of CPU. An equation has been derived for the normal derivative of the pressure on the body surface, which becomes zero when the body surface has no curvature. A condition for bisection of a droplet by the wedge has been introduced, which seems to be rational and provides converged results.

References

1. Z. N. Dobrovol'skaya, On some problems of similarity flow of fluid with a free surface, *J. Fluid Mech.* **36** (1969) 805–829.

2. R. Zhao and O. Faltinsen, Water entry of two-dimensional bodies, *ibid.* **246** (1993) 593–612.
3. C. H. Lu, Y. S. He and G. X. Wu, Coupled analysis of nonlinear interaction between fluid and structure during impact, *J. Fluids Struct.* **14** (2000) 127–146.
4. G. X. Wu, H. Sun and Y. S. He, Numerical simulation and experimental study of water entry of a wedge in free fall motion, *ibid.* **19** (2004) 277–289.
5. G. X. Wu and R. Eatock Taylor, The coupled finite element and boundary element analysis of nonlinear interactions between waves and bodies, *Ocean Engng* **30** (2003) 387–400.
6. G. X. Wu, Numerical simulation of water entry of twin wedges, *J. Fluids Struct.* **22** (2006) 99–108.
7. E. Cumberbatch, The impact of a water wedge on a wall, *J. Fluid Mech.* **7** (1960) 353–374.
8. G. X. Wu, Fluid impact on a solid boundary, *J. Fluids Struct.* **23** (2007) 755–765.
9. S. D. Howison, J. R. Ockendon, J. M. Oliver, R. Purvis and F. T. Smith, Droplet impact on a thin fluid layer, *J. Fluid Mech.* **542** (2005) 1–23.
10. R. Purvis and F. T. Smith, Droplet impact on water layers: post-impact analysis and computations, *Philos. Trans. R. Soc.* A **363** (2005) 1209–1221.
11. M. Greenhow, T. Vinje, P. Brevig and J. Taylor, A theoretical and experimental study of capsize of Salter's duck in extreme waves, *J. Fluid Mech.* **118** (1982) 221–239.
12. W. M. Lin, J. N. Newman and D. K. Yue, Nonlinear forced motions of floating bodies, *Proceeding of 15th Symposium of Naval Hydrodynamics* (ONR, National Academy Press, Washington, 1985).
13. G. X. Wu and R. E. Taylor, Time stepping solution of the two dimensional non-linear wave radiation problem, *Ocean Engng* **22** (1995) 785–798.
14. G. X. Wu, Hydrodynamic force on a rigid body during impact with liquid, *J. Fluids Struct.* **12** (1998) 549–559.